Journal of Biomedical Informatics **34,** 74–84 (2001)
doi:10.1006/jbin.2001.1003, available online at http://www.idealibrary.com on IDEAL®

g

Jeannette L. Herring and Benoît M. Dawant[2]

Department of Electrical and Computer Engineering, Vanderbilt University, Nashville, Tennessee 37235

Received November 28, 2000; published online June 6, 2001

This work proposes the use of surface-based registration to automatically select a particular vertebra of interest during surgery. Manual selection of the correct vertebra can be a challenging task, especially for closed-back, minimally invasive procedures. Our method uses shape variations that exist among lumbar vertebrae to automatically determine the portion of the spinal column surface that correctly matches a set of physical vertebral points. In our experiments, we register vertebral points representing posterior elements of a single vertebra in physical space to spinal column surfaces extracted from computed tomography images of multiple vertebrae. After registering the set of physical points to each vertebral surface that is a potential match, we then compute the standard deviation of the surface error for each registration trial. The registration that corresponds to the lowest standard deviation designates the correct match. We have performed our current experiments on two plastic spine phantoms and two patients.

1. INTRODUCTION

Improving the feasibility of image-guided back surgery by performing a real-time registration of vertebrae in different image modalities or in image and physical space is an active research area. Several clinical studies have been done to show that the technique is a valid approach for the insertion of pedicle screws [1, 3, 4, 7, 19, 21]. Image-guided surgical techniques have also been used successfully to perform lumbar discectomies [15, 18] and spinal biopsies [8, 22].

An important premise of these clinical studies is that the physical points must be collected from the correct vertebra, that is, from the vertebra that is involved in the surgical procedure. This intraoperative identification of the correct vertebra can be difficult, especially for minimally invasive procedures. It requires the surgeon to count vertebrae by feeling spinous processes through the skin, a procedure that is complicated by the presence of fatty tissues. Because this manual identification process introduces the possibility of error, it would be helpful to have a registration algorithm that could automatically locate the vertebra of interest. A potential method of automatic identification is to register vertebral surface points acquired intraoperatively to multiple vertebrae within the surface of a spinal column generated from CT scans acquired preoperatively. Because each vertebra has a slightly different shape, measures related to the quality of the registration process should indicate the vertebral surface in the image volume to which the physical point set corresponds.

In addition to the clinical studies that have been done in the area of image-guided vertebral surgery, several technical studies have been performed to investigate various methods

[1]Parts of this work have been presented at the MICCAI conference in September 1999 and at the SPIE conference in February 2000.

[2]To whom correspondence should be addressed at, Box 1662, Station B, Vanderbilt University, Nashville, TN 37235. E-mail: dawant@vuse.vanderbilt.edu.

1532-0464/01 $35.00

of vertebral segmentation and registration. In particular, Lavallée and colleagues have done a substantial amount of work in this area. Their studies show that submillimetric registration accuracy can be achieved between points obtained intraoperatively and surfaces extracted preoperatively from CT images. In these studies, intraoperative points are obtained using a variety of methods, including an optically tracked ultrasound probe, a three-dimensional (3-D) pointer, and projection X-ray images. Preoperative surfaces are generated from CT images using modified snake and spline techniques [13]. Points are registered to surfaces by minimizing the energy required to make projection lines from 2-D contours tangent to the 3-D surface when using X-ray images and by applying more traditional surface-based techniques when using 3-D methods of point collection [10, 11]. Results reported so far using automatic or semiautomatic surface generation techniques have been achieved primarily on single isolated vertebrae [12].

Our research demonstrates that surface-based registration methods can be used not only to register points from a single vertebra to a surface that contains multiple vertebrae, but also to identify which vertebral surface in a CT image volume best corresponds to the physical point set. To perform the surface-based registration, we use a method based upon the iterative closest point algorithm developed by Besl and McKay [2]. To segment the vertebral surface, we use an improved version of the fully automatic marching cubes algorithm proposed by Lorensen and Cline [14]. The modified marching cubes algorithm automatically computes a triangle set representing the closest approximation to an isosurface that is characterized by a specific intensity value. Of course, this segmentation method results in the inclusion of overlapping parts of neighboring vertebrae in addition to the vertebra of interest, but the extraneous surface information does not appear to be a problem for the surface-based registration process we use.

2. METHODS

2.1. Image Acquisition

We have performed our experiments on two plastic phantoms of the spine and two sets of patient data. The first phantom, which we have designated Phantom I, is a life-size model of the entire spinal column. The second phantom, designated Phantom II, is a life-size model of the lumbar portion of the spinal column. Both phantoms are molded out of vinyl ester plastic and are manufactured by the Carolina Biological Supply Company in Burlington, North Carolina. The first patient scan, designated Patient I, is a scan of the entire lumbar portion of the spinal column with no known pathologies. The second patient scan, designated Patient II, is a scan of the L1 through L4 portion of a spinal column damaged by osteoporosis.

CT scans of the two phantoms were obtained using a Philips Tomoscan AV scanner. Three scans with slice thicknesses of 2, 3, and 5 mm were taken for each phantom. For both phantoms, the first image volume contains 70 slices with a slice thickness of 2 mm; the second contains 47 slices with a slice thickness of 3 mm; and the third contains 29 slices with a slice thickness of 5 mm. For each image set, every slice has 512×512 voxels with voxel dimensions in millimeters of $0.625 \times 0.625 \times$ the slice thickness. Phantom I was placed in the scanner to ensure that complete images of vertebrae L1 and L2 were obtained, and Phantom II was placed in the scanner to ensure that complete images of vertebrae L3, L4, and L5 were obtained.

A CT scan of all five lumbar vertebrae was obtained for Patient I using the Philips scanner. The patient image volume contains 37 slices with a slice thickness of 5 mm. Every slice has 512×512 voxels with voxel dimensions in millimeters of $0.586 \times 0.586 \times 5$. A CT scan of L1 through L4 was obtained for Patient II using the Philips scanner. The Patient II image volume contains 32 slices with a slice thickness of 3 mm. Every slice has 512×512 voxels with voxel dimensions in millimeters of $0.605 \times 0.605 \times 3$.

All CT image volumes used in this study were acquired as stacks of image slices with no interslice gap or slice overlap. The gantry tilt angle during image acquisition was zero.

2.2. Triangulated Surface Extraction

A triangle set representation of the surface of the spinal column was automatically extracted from each CT scan using an independently implemented version of the classic marching cubes method developed by Lorensen and Cline [14]. The number of triangles in the resulting mesh was reduced using the decimation algorithm from the commercially available Visualization Toolkit (VTK) [20].

The only parameter required by the marching cubes algorithm is an intensity value. This algorithm is well suited to the extraction of bone surfaces in CT images, since the intensity level of bone is generally an order of magnitude greater than the intensity levels of all other materials and thus provides a near-ideal isosurface. Hounsfield numbers of the plastic phantoms range from approximately 600 to

approximately 800, with Phantom II having a slightly higher Hounsfield number than Phantom I. The Hounsfield number of the air surrounding the phantom is −1024. There is an offset of 1024 introduced into the intensity values due to the method used to transfer the scans from the CT machine, resulting in average intensity values of about 1600 to 1800 for the plastic and 0 for the surrounding air. Thus, isosurfaces were created for the phantom scans at the intermediate intensity values of 800 for Phantom I and 900 for Phantom II.

For the two patient scans, the offset of 1024 was not introduced during image transfer. Intensity values are approximately 600 and 0 for vertebral bone and surrounding tissue, respectively, and the isosurface for Patient I was created at an intermediate intensity value of 175. Because of the lower bone density due to osteoporosis in Patient II, the isosurface for this second patient CT scan was created at an intermediate intensity value of 100.

2.3. Surface Point Identification

For the two phantoms, physical space coordinates of approximately 900 surface points were acquired for each vertebra using a three-dimensional spatial localizer (3DSL) consisting of a probe and an Optotrak 3020 system (Northern Digital, Ontario, Canada). These points were collected by sweeping the 3DSL over the vertebral surface rather than by individually touching each point. With this method, hundreds of points can be acquired in a matter of seconds. For the patients, simulation points representing physical space were drawn manually on the CT image sets. The processes of physical point collection and simulation point identification were performed by an engineering graduate student with advice from a general surgeon. To use this method in a clinical setting, we propose to extract physical points from ultrasound scans taken in the operating room. We are currently investigating the feasibility of this strategy.

For each phantom and patient vertebra, the collected surface points cover the entire posterior area from the tips of the transverse processes, across the superior and inferior articular facets, through the central laminar regions, and to the sides and tip of the spinous process. In addition to using the entire set of 900 points to perform surface-based registration in our experiments, we also use a subset of approximately 300 points covering only the central laminar regions and the tip of the spinous process. In previous work, we have shown that this particular subset of points (designated point set CE) provides sufficient information for accurate surface-based registration [5, 6]. Point set CE is also of clinical interest, since the central laminar regions and the tip of the spinous process tend to be more easily accessible than other regions of the vertebral surface. Because point set CE performs well in the task of surface-based registration for individual vertebrae, our current investigation of automatic vertebral identification compares the results of using point set CE with the results of using the entire set of 900 points (designated point set Total).

2.4. Registration

We perform surface-based registration of physical points from each lumbar vertebra to the spinal column surfaces extracted from the CT scans of Phantom I, Phantom II, and the two patient scans. That is, we attempt to register physical points collected from vertebra L1 to surfaces corresponding to all five lumbar vertebrae, and we repeat the process for L2 through L5. (Since the Patient II scan contains only vertebrae L1 through L4, its analysis includes only those four lumbar vertebrae.) The extracted spinal column surfaces contain multiple vertebrae, so our registration trials address the question of whether the vertebral surface that correctly matches our physical (or simulation) point set can be selected out of several choices.

To perform our registration trials, we use an independent implementation [16] the iterative closest point registration algorithm of Besl and McKay [2]. The method is a two-step process. First, the closest point on one surface is computed for each point in a set of points representing the other surface. (In this study, the first surface is a triangle set representation of the bone surface in the CT image, and the point set representation of the second surface is a set of physical-space surface points or simulation points representing physical space.) Second, a transformation is determined by registering these two point sets. This process is iterated until some stopping criterion is satisfied. The method converges to a local minimum of the cost function, which is the root-mean-square distance between the corresponding points at the last iteration. Because the physical-space surface points we record are the positions of the center of the ballpoint tip of the 3DSL, the recorded surface points are displaced from the actual surface by the radius of the tip. We use the method described by Maurer and colleagues to correct for this displacement [17].

Because of the possibility of convergence to a local minimum that is not the correct solution, the algorithm works best when it is initialized with rotations and translations that are close to the exact solution. In this work, the initial registration for correctly matched vertebral points and surfaces is computed by aligning the principal axes of the

physical surface points and the CT image surface. The initial registration for mismatched points and surfaces is computed by translating the correctly matched initial position along the spinal column. We use a translation of approximately ± 30 mm per vertebra through which the correct position is displaced. This method of finding different initial positions along the spinal column should translate directly into clinical work: The principal axes transformation can be used to find the initial position of the vertebra of interest, and that position can then be translated up and down the spinal column to test whether the chosen vertebra is actually the correct one.

2.5. Error Computation

In this paper, we report our results in terms of surface error, which is computed as the RMS distance of the registered point set from the surface. It is important to distinguish surface error from registration error, since we have found that surface error is generally not a good predictor of registration error. However, our method of assessing registration error requires the comparison of surface-based registration results with a gold standard, and we use point-based registration results obtained using fiducial markers as our gold standard. Since this work investigates mismatched vertebral registrations, there is no associated gold standard; thus, we have chosen the less accurate measure of RMS surface error to assess our results. While this measure of error is less meaningful in the overall sense of assessing registration accuracy, we find that it is useful for our purposes of automatically distinguishing between correct and incorrect pairs of vertebral points and surfaces.

In addition to investigating RMS surface error, we also explore the standard deviation of RMS surface error. That is, we compute the standard deviation of the set of numbers obtained by measuring individual distances from each physical point to the corresponding closest point on the surface.

3. RESULTS

3.1. Triangulated Surfaces

Figure 1 shows triangulated surfaces extracted from the 2-mm CT scan of Phantom II and from the 5-mm CT scan of Patient I. From top to bottom, Fig. 1a shows part of L2 on Phantom II, vertebrae L3, L4, and L5 (which can be identified by the fiducial markers in the right central laminar regions), and part of the sacrum. From top to bottom, Fig. 1b shows part of a thoracic vertebra on the patient, the five lumbar vertebrae, and part of the sacrum. Each image contains some extraneous information, but the posterior elements of the vertebrae are clearly delineated in all cases. Similar surfaces exist for the 3- and 5-mm phantom scans and for Phantom I and Patient II.

In Fig. 1, note that the posterior point sets which we have

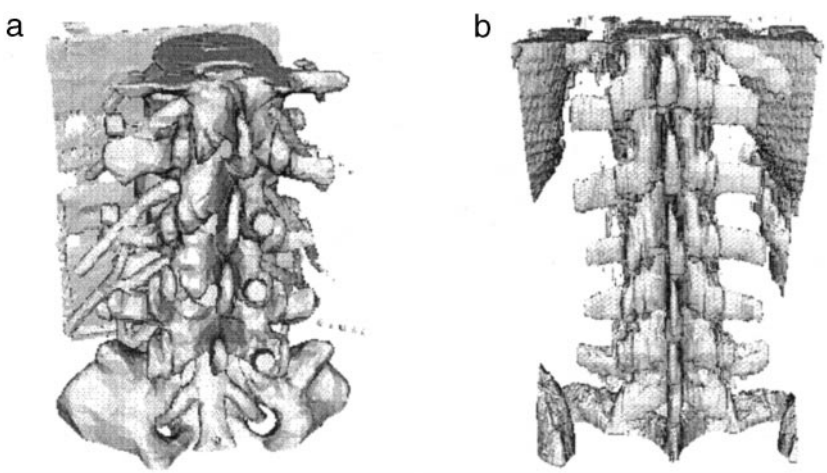

FIG. 1. (a) Surface of spinal column extracted from 2-mm CT scan of Phantom II. The surface contains parts of L2 and the sacrum and all of L3, L4, and L5. (b) Surface of spinal column extracted from the 5-mm patient CT scan. The surface contains part of a thoracic vertebra, all five lumbar vertebrae, and part of the sacrum.

chosen to use in our registration trials have similar shapes, especially for neighboring vertebrae and especially for point set CE. Also, note that the markers visible in Fig. 1a are not used in this particular experiment; they are related to other registration trials which we have conducted.

3.2. Phantom Registration Trials

Figure 2 shows the RMS surface errors obtained by registering point set CE to the surfaces extracted from the 2-mm phantom CT scans. (Recall that L1 and L2 are extracted from the scan of Phantom I, and L3, L4, and L5 are extracted from the scan of Phantom II.) Each bar represents the result of registering the physical point set designated by the legend to the vertebral surface shown along the *x* axis. As noted under Methods, the surface points are displaced from the actual surface by the radius of the ballpoint tip of the 3DSL, which is 0.5 mm. Our program to compute surface distance does not correct for this displacement, so the RMS surface error should be 0.5 mm in Fig. 2 for a "perfect" fit.

Without exception, Fig. 2 shows that the correctly matched points and surfaces yield the lowest RMS surface errors. However, it is interesting to note that the RMS surface errors for mismatched vertebrae are also consistently low, even when the two vertebrae being matched have quite different shapes, as is the case for L1 and L5 in this particular experiment. In fact, certain incorrect matches provide surface errors that are not dramatically higher than the errors generated by correct matches. For example, consider the results of registering points from L1, L2, and L3 to the surface of L2. The L2-to-L2 match has the lowest RMS surface error at 0.56 mm, but both the L1-to-L2 and L3-to-L2 mismatches have surface errors of 0.86 mm, which is also a relatively low value.

The fact that RMS surface errors are relatively low for mismatched points and surfaces suggests that this error may not be the best indicator of a vertebral mismatch. This observation led us to examine the standard deviation of surface error as a possible indicator. Figure 3a shows the standard deviation for each registration trial shown in Fig. 2. As before, each bar represents the registration result obtained for the physical point set designated by the legend and the vertebral surface shown along the *x* axis. Again, the correctly matched points and surfaces yield the lowest standard deviations in all cases. However, the spread is greater in this chart, suggesting that the standard deviation is a better predictor of a correct match than the RMS surface error.

Because standard deviation of surface error provides greater differentiation between correct and incorrect matches, we will present results in terms of standard deviation for the remainder of this paper. Subsequent results show the effect of increasing slice thickness and the effect of using point set Total rather than point set CE. (Recall that point set Total covers the entire posterior vertebral surface and point set CE covers the central laminar regions and the tip of the spinous process.)

Figures 3b and 3c show standard deviations obtained by registering point set CE to surfaces extracted from the 3- and 5-mm phantom CT scans, respectively. In Fig. 3b, correctly matched points and surfaces yield the lowest standard deviations in all cases. In Fig. 3c, correctly matched points and surfaces yield the lowest standard deviations for vertebrae L1, L2, L3, and L5. However, the incorrect match of L5 points to the L4 surface provides the lowest standard deviation for L4. Figure 4c shows that this problem can be solved by using point set Total, a finding that will be explained under Discussion.

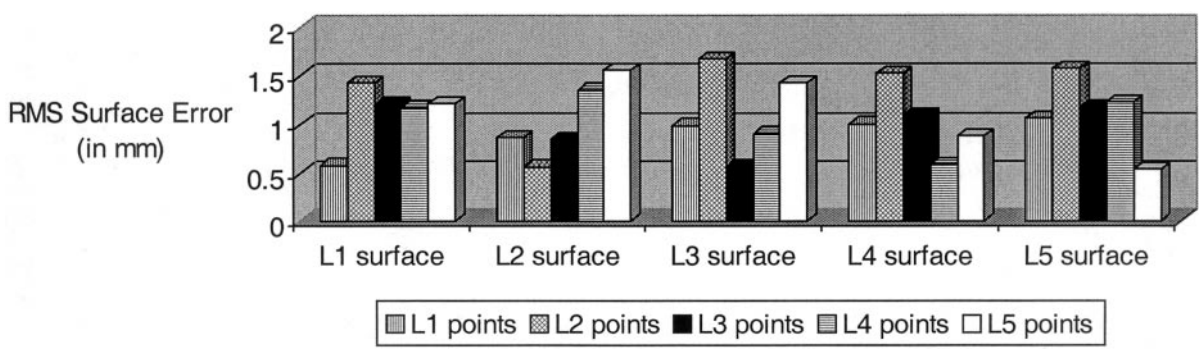

FIG. 2. RMS surface errors for physical points sets shown in the legend registered to vertebral surfaces shown along the *x* axis. All point sets are set CE. Surfaces for L1 and L2 are portions of the surface extracted from the 2-mm Phantom I CT scan, and surfaces for L3, L4, and L5 are portions of the surface extracted from the 2-mm Phantom II CT scan.

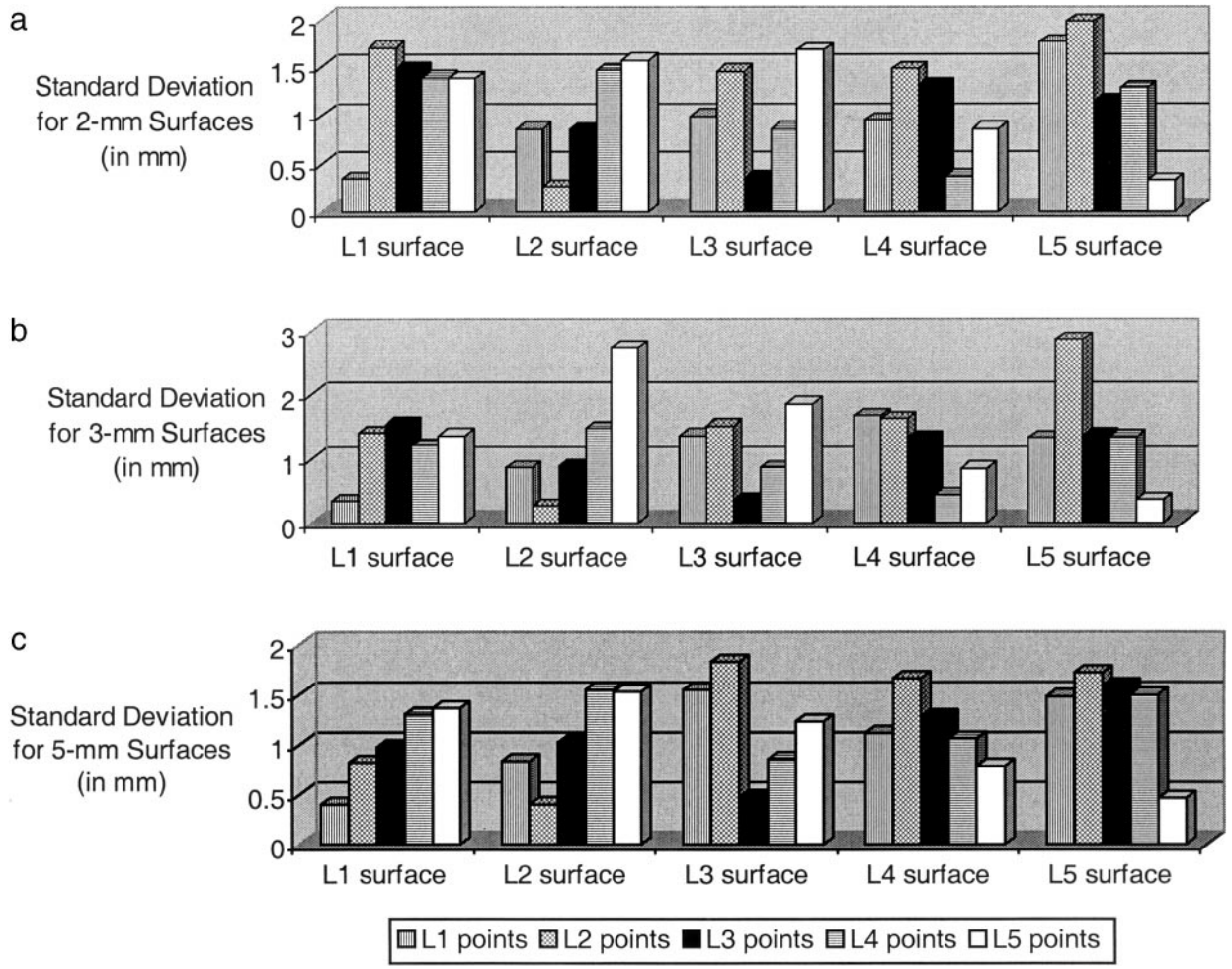

FIG. 3. Standard deviations of surface errors for physical point sets shown in the legend registered to vertebral surfaces shown along *x* axis. All points set are set CE. Surfaces for L1 and L2 are portions of the surface extracted from the (a) 2-mm, (b) 3-mm, and (c) 5-mm Phantom I CT scan, and surfaces for L3, L4, and L5 are portions of the surface extracted from the (a) 2-mm, (b) 3-mm, and (c) 5-mm Phantom II CT scan.

Figures 4a, b, and c show standard deviations obtained by registering point set Total to surfaces extracted from the 2-, 3-, and 5-mm phantom CT scans, respectively. In these figures, correctly matched points and surfaces yield the lowest standard deviations in all cases. A comparison of Fig. 4 with Fig. 3 shows that point set Total provides greater differentiation between correct and incorrect matches than point set CE. However, note that results for all point sets are quite close for L4 in Fig. 4c, which corresponds to the incorrectly predicted match for point set CE registered to the 5-mm data set in Fig. 3c. Again, these observations will be explained under Discussion.

3.3. Patient Registration Trials

Figure 5 shows standard deviations obtained by registering point sets CE and Total to surfaces extracted from the 5-mm CT scan of Patient I. For point set CE, shown in Fig. 5a, correctly matched points and surfaces yield the lowest standard deviations for vertebrae L1, L2, L3, and L5. However, the incorrect match of L3 points to the L4 surface provides the lowest standard deviation for L4. Also, results for all point sets are quite close for L4 and L5, which leads to poor certainty even for the correctly matched L5. These results correspond to the results for the 5-mm phantom trials and will be explained under Discussion. For point set Total,

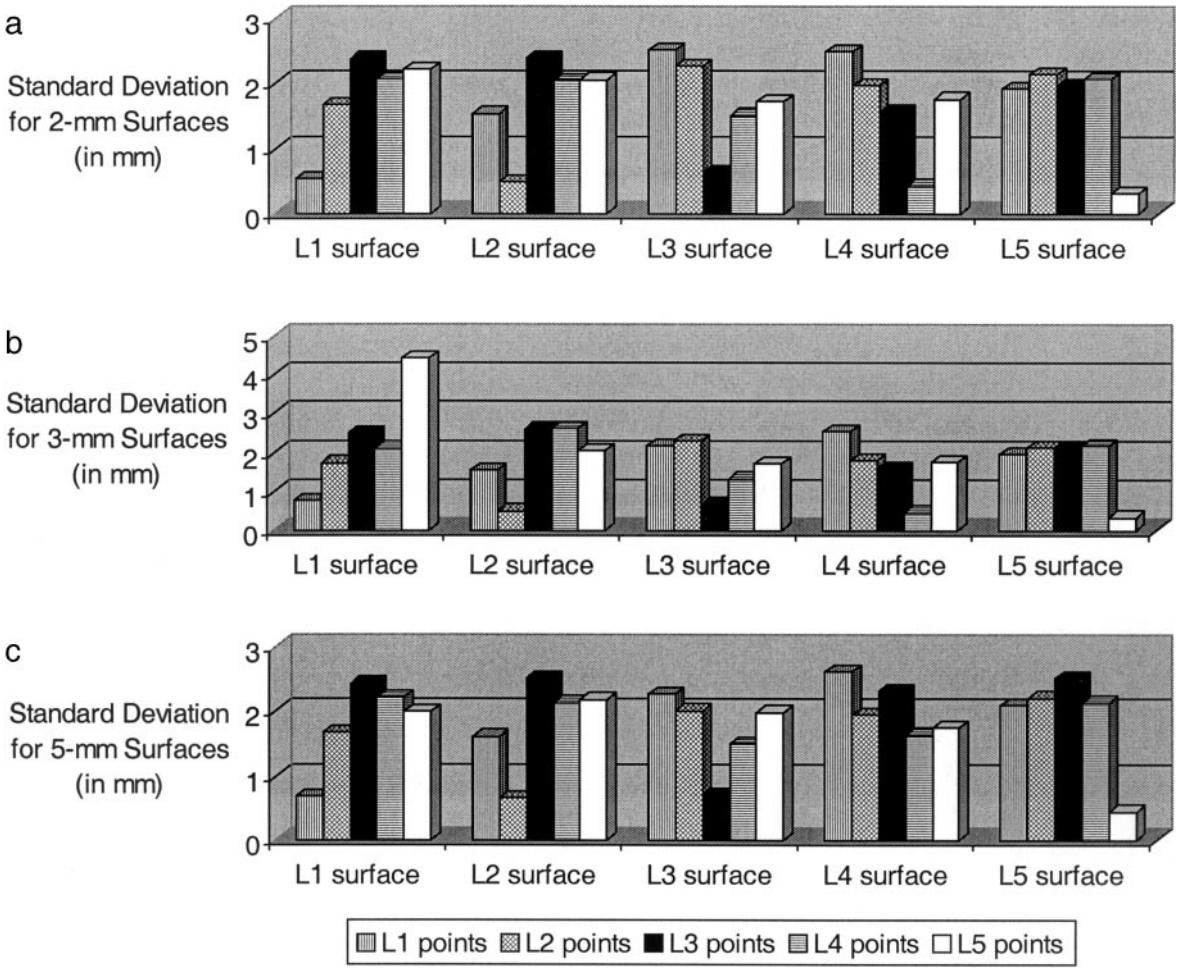

FIG. 4. Standard deviations of surface errors for physical point sets shown in the legend registered to vertebral surfaces shown along the *x* axis. All point sets are set Total. Surfaces for L1 and L2 are portions of the surface extracted from the (a) 2-mm, (b) 3-mm, and (c) 5-mm Phantom I CT scan, and surfaces for L3, L4, and L5 are portions of the surface extracted from the (a) 2-mm, (b) 3-mm, and (c) 5-mm Phantom II CT scan.

shown in Fig. 5b, correctly matched points and surfaces yield the lowest standard deviations in all cases.

Figure 6 shows standard deviations obtained by registering point sets CE and Total to surfaces extracted from the 3-mm CT scan of Patient II. In both cases, correctly matched points and surfaces yield the lowest standard deviations for all four vertebrae. However, differentiation between correct and incorrect matches is greater when point set Total is used, an observation that supports trends noted for other data sets. Recall that vertebra L5 is not included in the results, since the original CT scan for Patient II does not contain L5 (as noted under Methods).

4. DISCUSSION

It is not surprising that the correct match yields the lowest RMS surface error in Fig. 2, but it is perhaps rather unexpected to find such small surface errors for mismatched vertebrae. This finding is due to fact that the registration algorithm is designed to minimize distance between the point set and the surface, the very distance which also serves as our definition of surface error. Because the behavior of the registration algorithm is controlled by point-to-surface distance, this distance is not a good assessment of registration

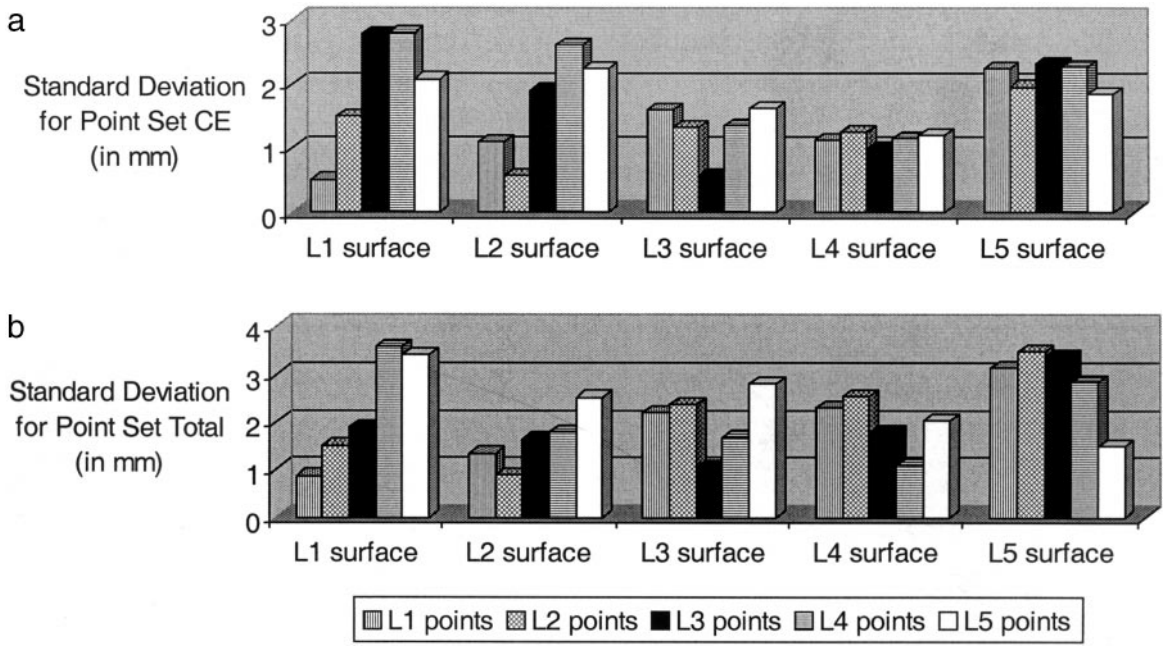

FIG. 5. Standard deviations of the surface errors for simulation point sets shown in the legend registered to vertebral surfaces shown along the *x* axis. All point sets are (a) set CE and (b) set Total, and all surfaces are portions of the surface extended from the 5-mm CT scan of Patient I.

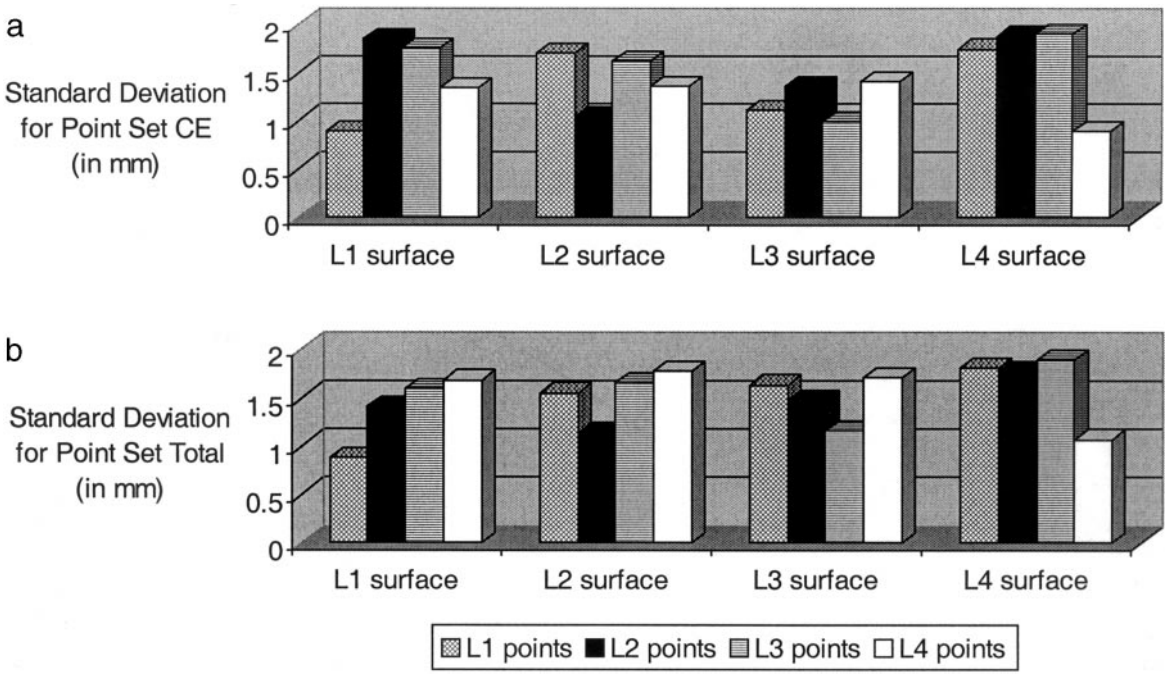

FIG. 6. Standard deviations of surface errors for simulation point sets shown in the legend registered to vertebral surfaces shown along the *x* axis. All point sets are (a) set CE and (b) set Total, and all surfaces are portions of the surface extracted from the 3-mm CT scan of Patient II.

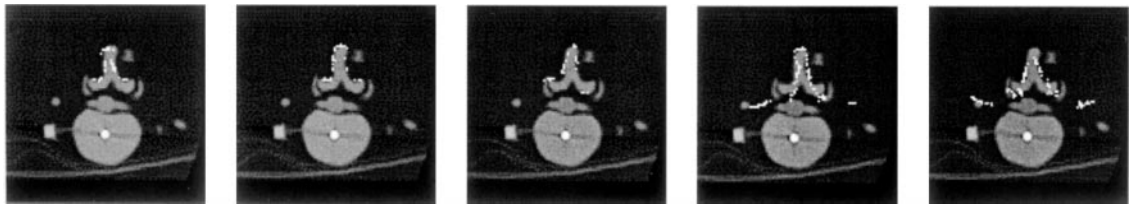

FIG. 7. Visual results of registering all five point sets to the surface of vertebra L2 on Phantom I. From left to right, points from L1 through L5 are shown on a single slice of the 2-mm CT image set of L2. Points are projected onto the closest 2-mm plane for plotting.

accuracy—as already noted under Methods. Figures 7 and 8 illustrate this fact by showing the results of registering all five point sets (L1 through L5, from left to right) to the surface of vertebra L2. Figure 7 shows results for a single slice of the Phantom I CT image set with 2-mm slice spacing, and points are projected onto the closest 2-mm plane for plotting. Figure 8 shows results for a single slice of the Patient I CT image set, and points are projected onto the closest 5-mm plane for plotting.

In Fig. 7, note that the registered points for L1, L2, and L3 do indeed lie close to the surface of L2, as the numbers in Fig. 2 indicate. However, points representing L1 show that its spinous process is slightly narrower and shorter than the spinous process of L2, resulting in a registration that places certain regions of the point set slightly inside the surface. Also, points in the right central laminar region of L3 are incorrectly registered to the inner surface of the spinal canal, rather than to the posterior vertebral surface. This misregistration and its resulting small RMS surface error provide an excellent example of the difficulty of determining registration accuracy by looking solely at surface error. Points for L4 and L5 are quite seriously misregistered, due to the increasingly different shapes of the vertebrae. Compared to L2, vertebrae L4 and L5 both have longer spinous processes and broader laminar regions. The larger RMS surface errors reported in Fig. 2 for L4 and L5 reflect this higher degree of misregistration, but they are still rather low due to the fact that many points are close to some surface. For example, points are registered to the inner surface of the spinal canal (as noted previously for the L3-to-L2 misregistration), the articular facets of the neighboring vertebra, and even the small nerves to the left and right of the vertebral

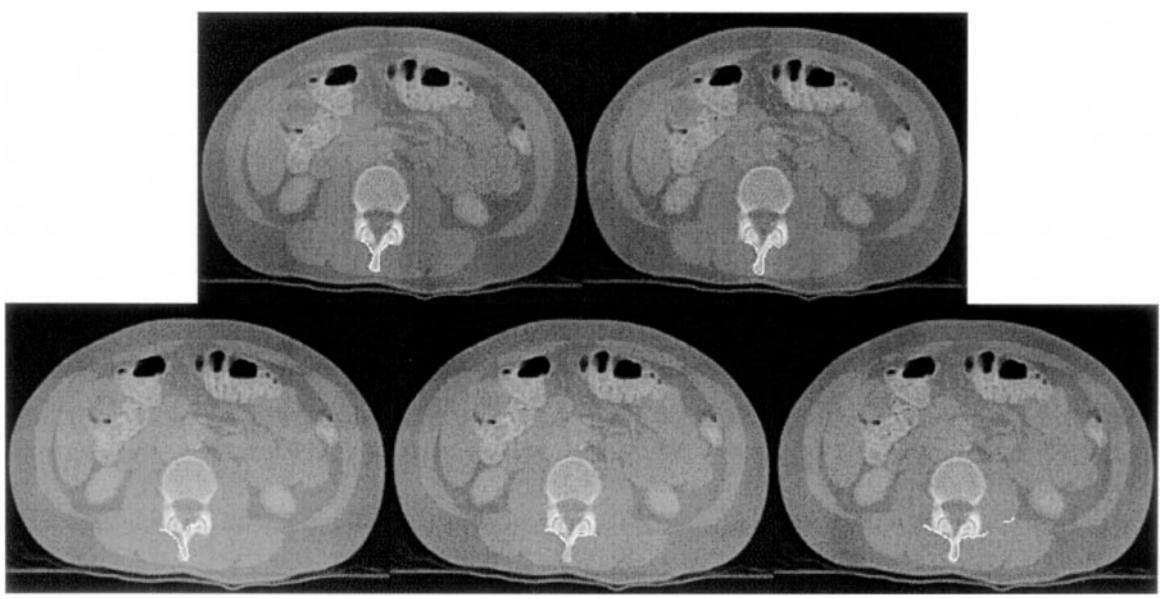

FIG. 8. Visual results of registering all five point sets to the surface of vertebra L2 on Patient I. From left to right on the top row, points from L1 and L2 are shown on a single slice of the CT image set of L2. From left to right on the bottom row, points from L3 through L5 are shown on the same slice of the CT image set of L2. Points are projected onto the closest 5-mm plane for plotting.

body. Similar statements can be made regarding the patient data in Fig. 8, although some points are slightly harder to see. The L1-to-L2 mismatch looks particularly good in this figure, but a careful examination of the shape of the spinous process tip for L2 will show that the L2-to-L2 match is indeed the correct one.

Figures 7 and 8 also help to explain our finding that standard deviation of surface error is a better predictor of a correct match than RMS surface error itself. Visual examination of the misregistered cases in these figures shows that the entire set of points is, on average, close to some surface. However, the point-to-surface distance is much less consistent for individual points, resulting in a larger standard deviation. For the correctly registered case, the excellent match between the shape of the point set and the shape of the surface results in a much more consistent distance between the points and the surface, or in other words, a smaller standard deviation.

An additional point of discussion is required to explain our finding in Figs. 3c and 5a that the method fails for vertebra L4 when the combination of point set CE and a surface extracted from a 5-mm CT scan is used. This failure is caused by the fact that there is not enough shape information present to distinguish between correct and incorrect matches. Additional shape information can be obtained either by increasing information in the point set (by using point set Total, for example) or by increasing information in the surface (by using a surface extracted from a CT scan with smaller slice spacing). The preferred method of increasing shape information is to use a surface extracted from a CT scan with smaller slice spacing, to allow for increased spatial resolution in the direction of slice thickness. A comparison of Fig. 3c with Figs. 3b and 4c supports this preference. These figures correct the error in Fig. 3c by making use of increased information in the extracted surface (in Fig. 3b) and increased information in the point set (in Fig. 4c). However, the correction is more dramatic with the additional surface information in Fig. 3b, which allows the correct match to be selected with greater certainty. In Fig. 4c, increased shape information in the point set can barely compensate for the lack of accurate shape information in the surface, which suggests that more detailed surface information is needed.

For the patient studies, a comparison of Figs. 5a and 6a shows that the correction caused by using an image set with a smaller slice spacing is not as pronounced as it is for the phantom studies. However, this comparison must be made with caution, as the two image sets reflect different patients. In other aspects of our work, we have noted that the patient with osteoporosis presents some unique challenges for our surface-based registration method because the lower bone density makes it more difficult to automatically extract a viable isosurface from the CT image set. Thus, gains obtained by the smaller slice spacing are partially offset by the difficulty in distinguishing an accurate isosurface of the spinal column.

It may be possible to improve the robustness of our identification process by taking certain additional information into account. As noted previously, mismatched pairs of vertebral points and surfaces frequently involve points being incorrectly registered to the inner surface of the spinal canal or to nerves that are some distance from the vertebra of interest. It would be relatively easy to declare certain registration results out of bounds by making an *a priori* determination of regions in the scan that do not contain posterior surfaces. For the examples shown in Figs. 7 and 8, taking this additional information into account would allow elimination of L3, L4, and L5 as possible matches for L2 on the phantom and elimination of L3 and L5 as possible matches for L2 on the patient. Another possibility is to use a different surface extraction method, particularly in difficult cases such as the osteoporotic Patient II.

5. CONCLUSION

Our experiments show that the standard deviation of RMS surface error can be used to select the correct match between a set of vertebral surface points collected in physical space and a surface of the spinal column extracted from a CT scan of multiple vertebrae. The method has been tested on two patients: one with no known spinal column abnormalities and one with a pronounced case of osteoporosis. The method works for phantom and patient data using point set CE or Total registered to surfaces extracted from CT scans with slice spacings of 2 or 3 mm. The method also works for phantom and patient data using point set Total registered to surfaces extracted from CT scans with slice spacings of 5 mm. These findings suggest that sufficient shape information in either the extracted surface or the point set contributes to the success of this technique for intraoperative automatic vertebral identification.

ACKNOWLEDGMENTS

This work has been supported in part by an NDSEG fellowship awarded through the Office of Naval Research and by NIH Grant

5R01-G752798-03. The authors express appreciation to Alan Herline, M.D., who provided guidance in the selection of target point sets; to Diane Muratore, who assisted with physical point collection; and to Allen Jackson, who provided the CT scans used in our study.

REFERENCES

1. Amiot L-P, Labelle H, Deguise JA, Sati M, Brodeur P, Rivard C-H. Computer-assisted pedicle screw fixation: a feasibility study. Spine 1995; 20:1208–12.
2. Besl P, McKay N-D. A method for Registration of 3-D shapes. IEEE Trans Pattern Anal Mach Intell 1992; 14:239–56.
3. Carl AL, Khanuja HS, Sachs BL, Gatto CA, Vomlehn J, Vosburgh K, Schenck J, Lorensen W, Rohling K, Disler D. *In Vitro* simulation: early results of stereotaxy for pedicle screw placement. Spine 1997; 22:1160–4.
4. Foley KT, Smith MM. Imaged-guided spine surgery. Neurosurg Clin North Amer 1996; 7:171–86.
5. Herring JL, Dawant BM, Maurer CR, Jr, Muratore DM, Galloway RL, Jr, Fitzpatrick JM. Surface-based registration of CT images to physical space for image-guided surgery of the spine: a sensitivity study. IEEE Trans Med Imaging 1998; 17:743–52.
6. Herring JL, Maurer CR, Jr, Dawant BM. Sensitivity analysis for registration of vertebrae in ultrasound and computed tomography images. Proc SPIE Conf Image Proc 1998; 3338:95–106.
7. Kalfas IH, Kormos DW, Murphy MA, McKenzie RL, Barnett GH, Bell GR, Steiner CP, Trimble MB, Weisenberger JP. Application of frameless stereotaxy to pedicle screw fixation of the spine. J Neurosurg 1995; 83:641–7.
8. Kattapuram SV, Rosenthal DI. Percutaneous biopsy of the cervical spine using CT guidance. AJR Amer J Roentgenol 1987; 149: 539–41.
9. Deleted in proof.
10. Lavallée S, Szeliski R. Recovering the position and orientation of free-form objects from image contours using 3D distance maps. IEEE Trans Pattern Anal Mach Intell 1995; 17:378–90.
11. Lavallée S, Szeliski R, Brunie L. Anatomy-based registration of three-dimensional medical images, range image, X-ray projections, and three-dimensional models using octree-splines. In: Computer-integrated surgery: technology and clinical applications. Taylor, R., Lavallée, S., Burdea, G., and Mösges, R., editors. Boston: Academic Press, 1996; 115–43.
12. Lavallée S, Troccaz J, Sautot P, Mazier B, Cinquin P, Merloz P, Chirossel J-P. Computer-assisted spinal surgery using anatomy-based registration. In: Computer-integrated surgery: technology and clinical applications. Taylor R, Lavallée S, Burdea G, Mösges R, editors. Boston: Academic Press, 1996; 425–49.
13. Leitner F, Marque I, Lavallée S, Cinquin P. Dynamic segmentation: finding the edge with snake splines. In: "Curves and surfaces" Laurent PJ, Le Méhauté A, Schumaker L. L, editors. Boston: Academic Press, 1991; 279–84.
14. Lorensen WE, Cline HE. Marching cubes: a high resolution 3D surface construction algorithm. Comput Graphics 1987; 21[4]: 163–69.
15. Mathews HH, Evans MT, Molligan HJ, Long BH. Laparoscopic discectomy with anterior lumbar interbody fusion. Spine 1995; 20:1797–802.
16. Maurer CR, Jr, Aboutanos GB, Dawant BM, Maciunas RJ, Fitzpatrick JM. A method for registration of 3-D images using multiple geometric features. IEEE Trans Med Imag 1996; 15:836–49.
17. Maurer CR, Jr, Maciunas RJ, Fitzpatrick JM. Registration of head CT images to physical space using a weighted combination of points and surfaces. IEEE Trans Med Imag 1998; 17:753–61.
18. Mayer HM, Brock M. Percutaneous endoscopic discectomy: surgical technique and preliminary results compared to microsurgical discectomy. J Neurosurg 1993; 78:216–25.
19. Nolte L-P, Zamorano LJ, Arm E, Visarius H, Jiang Z, Berlemann U, Schwarzenbach O. Image-guided computer-assisted spine surgery: a pilot study on pedicle screw fixation. Stereotactic Funct Neurosurg 1996; 66:108–17.
20. Schroeder W, Martin K, Lorensen B. The visualization toolkit. Upper Saddle River, NJ: Prentice Hall, 1998.
21. Steinmann JC, Herkowitz HN, El-Kommos, H, Wesolowski DP. Spinal pedicle fixation: confirmation of an image-based technique for screw placement. Spine 1993; 18:1856–61.
22. Stringham DR, Hadjipavlou A, Dzioba RB, Lander P. Percutaneous transpedicular biopsy of the spine. Spine 1994; 19:1985–91.